Iron increases the susceptibility of multiple myeloma cells to bortezomib

Alessandro Campanella,[1] Paolo Santambrogio,[2] Francesca Fontana,[1] Michela Frenquelli,[3] Simone Cenci,[1] Magda Marcatti,[4] Roberto Sitia,[1,5] Giovanni Tonon,[3] and Clara Camaschella[1,5]

[1]Division of Genetics and Cell Biology; [2]Division of Neuroscience; [3]Division of Molecular Oncology; [4]Department of Hematology, San Raffaele Scientific Institute; and [5]Vita-Salute University, Milan, Italy

ABSTRACT

Multiple myeloma is a malignant still incurable plasma cell disorder. Pharmacological treatment based on proteasome inhibition has improved patient outcome; however, bortezomib-resistance remains a major clinical problem. Inhibition of proteasome functionality affects cellular iron homeostasis and iron is a potent inducer of reactive oxygen species and cell death, unless safely stored in ferritin. We explored the potential role of iron in bortezomib-resistance. We analyzed iron proteins, oxidative status and cell viability in 7 multiple myeloma cell lines and in plasma cells from 5 patients. Cells were treated with increasing bortezomib concentrations with or without iron supplementation. We reduced ferritin levels by both shRNA technology and by drug-induced iron starvation. Multiple myeloma cell lines are characterized by distinct ferritin levels, which directly correlate with bortezomib resistance. We observed that iron supplementation upon bortezomib promotes protein oxidation and cell death, and that iron toxicity inversely correlates with basal ferritin levels. Bortezomib prevents ferritin upregulation in response to iron, thus limiting the ability to buffer reactive oxygen species. Consequently, reduction of basal ferritin levels increases both bortezomib sensitivity and iron toxicity. In patients' cells, we confirmed that bortezomib prevents ferritin increase, that iron supplementation upon bortezomib increases cell death and that ferritin reduction overcomes bortezomib resistance. Bortezomib affects iron homeostasis, sensitizing cells to oxidative damage. Modulation of iron status is a strategy worth exploring to improve the efficacy of proteasome inhibition therapies.

Introduction

Multiple myeloma (MM) is a malignant disorder characterized by monoclonal proliferation of plasma cells in the bone marrow and by overproduction of circulating monoclonal immunoglobulin. Full-blown MM presents bone lesions sometimes accompanied by hypercalcemia, renal insufficiency and anemia. Anemia is caused by the pool of inflammatory cytokines released by plasma cells and the bone marrow microenvironment, and by the increased production of the serum hormone hepcidin.[1] The latter degrades the iron exporter ferroportin, causing iron retention in macrophages, enterocytes and hepatocytes. Although iron plays a role in the pathophysiology of anemia in MM,[1,2] its regulation has not been investigated in depth in malignant plasma cells.

To avoid iron toxicity, systemic and local iron homeostasis is tightly regulated.[3,4] Mammalian cells uptake iron from serum diferric transferrin (FeTf) through the endocytic pathway that involves Transferrin Receptor 1 (TfR1) for iron uptake and Divalent Metal Transporter 1 (DMT1) for iron release from endosome to cytosol. Cells may also uptake non-transferrin-bound iron probably through surface DMT1 or other not yet fully characterized transporters.[5] To avoid the detrimental Fenton reaction and ROS generation, excess iron is rapidly sequestered and safely stored by cytosolic ferritin, a shell protein formed by assembled L (FtL) and H (FtH) ferritin subunits.[6] Alternatively, excess iron is exported by ferroportin (Fpn). Depending on iron concentration, Iron Regulatory Proteins (IRP1 and IRP2) co-ordinately modulate iron protein levels post-transcriptionally by binding to Iron Responsive Elements (IREs) on mRNAs of TfR1, ferritin subunits and DMT1 and Fpn IRE-isoforms.[7] In synthesis, high iron reduces the IRP-IRE binding, promoting ferritin and ferroportin synthesis, and in parallel limits iron uptake by reducing TfR1 and DMT1, while low iron does exactly the opposite. Iron excess promotes IRP inactivation by iron-sulphur cluster insertion in the IRP1 molecule and inducing proteasomal degradation of IRP2 protein.

Bortezomib is a reversible inhibitor of the 26S proteasome, widely used to treat both newly diagnosed and relapsed/refractory MM patients. Bortezomib affects various signaling pathways[8] that promote death of malignant plasma cells; its introduction in the treatment of MM patients has significantly improved their outcome.[9] However, the drug has multiple side effects, the most severe being peripheral neuropathy. Moreover, several patients are intrinsically or become bortezomib-resistant.[10] With the aim of improving bortezomib efficacy, investigating iron metabolism looks promising: 1) iron is a powerful inducer of reactive oxygen species (ROS) and cell death; 2) the proteasome plays an important role in iron homeostasis[11] that may be altered by proteasome inhibitors. The proteasome mediates the iron-dependent degradation of IRP2 and in some cases of IRP1.[12] Moreover, increased TfR1 expression and iron uptake have

 doi:10.3324/haematol.2012.074872
The online version of this article has a Supplementary Appendix.
Manuscript received on July 26, 2012. Manuscript accepted on December 5, 2012.
Correspondence: camaschella.clara@hsr.it

been reported following proteasome inhibition in cells treated with H_2O_2 and nitric oxide generators.[13,14] Ferritin might undergo proteasomal degradation to recycle stored iron in cells pre-loaded with ferric ammonium citrate (FAC)[15] in conditions of decreased cell iron content[16,17] or in the presence of oxidative stress stimuli.[18]

Here we report the analysis of iron metabolism and the effects of iron manipulation in MM cell lines and primary cells of patients treated with bortezomib. We observed that the basal iron storage capacity of MM cell lines directly correlates with bortezomib resistance and that bortezomib sensitizes MM cells to iron toxicity. Manipulation of iron homeostasis might be a tool to increase the susceptibility of MM cells to the effect of bortezomib and to overcome bortezomib resistance.

Design and Methods

Cell culture and cellular extracts

Cell culture media and reagents were from Invitrogen (Karlsruhe, Germany) and from Sigma-Aldrich (St. Louis, MO, USA). Bortezomib was purchased from LC Laboratories (Wobun, MA, USA). Patient-derived plasma cells were purified from bone marrow aspirates by density gradient centrifugation and then by CD138 immunomagnetic positive selection (Miltenyi Biotec, Bergisch Gladbach, Germany). Samples from Patient 2 were collected both at diagnosis (sample a) and relapse (sample b). Informed consent was obtained in accordance with the Declaration of Helsinki and the approval for use of primary samples was obtained from the Institutional Review Board of the San Raffaele Scientific Institute. MM cell lines and primary cells were cultured in RPMI medium supplemented with 10% fetal bovine serum (FBS), 100 units/mL penicillin, 100 mg/mL streptomycin and 2 mM L-glutamine.

Cellular extracts were prepared as described in the *Online Supplementary Appendix*.

Iron manipulations

Iron removal was obtained by addition of deferoxamine (DFO; Biofutura Pharma, Milan, Italy). Ferric ammonium citrate (FAC), holo-transferrin (FeTf) (Sigma-Aldrich) and N-acetyl Cysteine (NAC) (Sigma-Aldrich) were used for iron loading experiments. FAC and ^{55}FeAC were prepared by mixing $FeCl_3$-HCl (Merk Millipore, Billerica, MA, USA) or $^{55}FeCl_3$-HCl (PerkinElmer, Monza, Italy) with citric acid at 1:2 ratios and then by adjusting pH to 7.4 with NH_4OH.

To estimate ferritin content in patients' cells, cellular extracts were incubated *in vitro* with a molar excess of ^{55}FeAC plus ascorbic acid. Then extracts were loaded without heating on sodium dodecylsulphate-polyacrylamide gel electrophoresis (SDS-PAGE) and exposed to autoradiography.

Cell viability

Cell viability was determined by measuring the reduction of 3-(4,5-dimethylthiazol-2-yl)-2,5-diphenyltetrazolium bromide (MTT) (Sigma-Aldrich). Briefly, cells were seeded in 96-well plates and assay performed on at least three wells for every condition. MTT was then added for 3 h at a final concentration of 0.25 mg/mL. Plates were centrifuged at 3200g for 5 min and the soluble fraction decanted. Crystal pellets were suspended in DMSO and absorbance read at 570 nM. Finally, results of viability were presented as percentage referred to untreated cells. Viable cells were assayed by Trypan Blue exclusion assay. Briefly, cells grown in triplicate were mixed 1:1 with Trypan Blue 0.4% (Invitrogen). The percentage of alive and dead cells was evaluated by counting each replica 3 times. Apoptosis and cell viability were determined by flow cytometry with AnnexinV-Propidium Iodide (AnV-PI) staining (BD Bioscience, San Diego, CA, USA), following the manufacturer's instruction. Data were analyzed by FCS-express 4 software (De Novo software, Los Angeles, CA, USA).

Oxidative status

Detailed protocols are reported in the *Online Supplementary Appendix*. Briefly, ROS were measured by incubating cells with the redox-sensitive probe CM-H2DCFDA (Invitrogen). Oxidized protein levels were evaluated using the Oxyblot Protein Oxidation Detection Kit (Merk Millipore) following the manufacturer's instructions.

Protein quantification, synthesis and turnover

Ferritin H was quantified by ELISA calibrated on the recombinant human FtH homopolymer using the rH02 monoclonal antibody, as previously described.[19]

TfR1, DMT1, Fpn, Catalase, Super Oxide Dismutase 1 (SOD1) and actin protein content were evaluated by WB after SDS-PAGE, as detailed in the *Online Supplementary Appendix*. To evaluate the rate of protein synthesis and turnover, cells were grown in cysteine and methionine-free RPMI medium (Invitrogen), supplemented with 100 mCi/mL [^{35}S]cysteine [^{35}S]methionine (Easy Tag Express Protein Labeling Mix, PerkinElmer) for 18 h. To assay for FtH and TfR1 synthesis cellular extracts were prepared immediately after labeling and immunoprecipitated using rH02 monoclonal antibody or anti-TfR1 (Invitrogen). To evaluate TfR1 turnover, cells were washed after labeling and then grown in RPMI medium for chase experiments. At the indicated times, soluble cellular extracts were prepared and immunoprecipitated using anti-TfR1. Precipitates were collected and loaded on SDS-PAGE. Finally gels were soaked with autoradiography enhancer (Amplify, GE Healthcare), dried and exposed.

All the analyses were performed on freshly prepared cellular extracts.

FTH silencing

To silence FTH expression, cells were infected with self-inactivating replication; incompetent viral particles and stable gene silencing was selected using the puromycin selectable marker. Viral particles were produced in packaging cells (HEK293T) by co-transfection with compatible packaging plasmids pMDLg/pRRE, pRSV.REV and pMD_2VSV.G together with Mission shRNA clone TRCN0000029429 (clone ID NM_002032.1-643s1c1) (Sigma-Aldrich) selectively targeting FTH mRNA. pLKO.1-puro Non-Target shRNA control plasmid was used as control.

Results

Ferritin levels directly correlate with bortezomib resistance in MM cell lines

We analyzed iron protein levels in a panel of 7 MM cell lines (MM.1S, KMS-18, RPMI-8226, U266, LP-1, KMS-26 and KMS-34). We evaluated the iron storage capacity by quantifying FtH, the iron import by measuring TfR1 and DMT1 and the iron export by measuring Fpn levels. Each MM cell line showed distinct and constant levels of FtH and TfR1 (*Online Supplementary Figures S1A* and *S2A*), while levels of DMT1 and Fpn were comparable among cells (*Online Supplementary Figure S2B* and *C*). To analyze the sensitivity to bortezomib, we determined the drug concentration sufficient to reduce cell viability by 50%

(IC50) in each cell line (*Online Supplementary Figure S1B*). We observed a wide range of sensitivity among the cell lines studied: U266 and RPMI-8226 were the most resistant (for the U266 the IC50 was not reached) and KMS-18 and MM.1S were the most sensitive cells (*Online Supplementary Figure S1B*). Interestingly, of the iron proteins analyzed only FtH directly correlated with IC50 (r^2=0.65) (*Online Supplementary Figures S1C* and *S2A-C*).

Since iron storage inside ferritin is a strategy to limit Fenton reaction and oxidative damage, we measured levels of other ROS buffering proteins, as catalase and SOD1. Levels of both enzymes were not correlated to bortezomib IC50 (*Online Supplementary Figure S2D* and *E*).

Iron supplementation increases cell death upon bortezomib in MM cell lines

Since ferritin levels correlate with bortezomib sensitivity, we evaluated the toxicity induced by iron supplementation in bortezomib-treated cells. For these experiments, we selected the sensitive MM.1S and KMS-18 cell lines, characterized by the lowest FtH levels, and the resistant RPMI-8226 and U266 cell lines, characterized by high FtH levels. The addition of both FeTf and FAC upon bortezomib favored cell death, as shown by the increase in late apoptoptic AnV-PI double positive cells (*Online Supplementary Figure S3A-D*). The addition of the antioxidant NAC abolished the effect of FeTf, but strongly increased FAC toxicity (*Online Supplementary Figure S3A-C*). In MM.1S and KMS-18, FAC toxicity was evident 18 h after iron supplementation, in U266 after 42 h, while in RPMI-8226 it was only slightly detectable (Figure 1A) (*Online Supplementary Figure S3A-D*).

To better define the mechanisms of iron toxicity, we measured ROS generation induced by FAC-NAC. The addition of iron induced ROS formation regardless of bortezomib in MM.1S and KMS-18, but not in U266 and in RPMI-8226 (Figure 1B). Cell damage, documented by enhanced oxidized proteins, was observed only in MM.1S and KMS-18 treated with both bortezomib and FAC-NAC (Figure 1C).

Bortezomib deregulates iron homeostasis in MM cell lines

The addition of bortezomib did not significantly affect FtH levels in all the cell lines tested, with the exception of U266, in which FtH increased approximately 1.5-fold (Figure 2A). In the same conditions, TfR1 increased approximately 2-fold in all cells (Figure 2B). Interestingly, bortezomib abolished the co-ordinated regulation of these proteins in response to iron manipulation. Indeed, FtH was not properly increased (Figure 2A) and TfR1 was not reduced (Figure 2B) by iron supplementation. This defective regulation occurred in all cells with the exception of U266, in which FtH was further increased by iron (Figure 2A). The iron export mechanism was not activated in bortezomib-treated cells, since Fpn levels remained unchanged in all experimental conditions (*Online Supplementary Figure S4A*). Similarly neither bortezomib nor iron affected catalase and SOD1 protein levels (*Online Supplementary Figure S4B and C*).

In an attempt to address the molecular mechanisms underlying the effect of bortezomib on iron proteins, we investigated the integrity of the IRP/IRE system that physiologically regulates TfR1 and ferritin levels. Bortezomib reduced IRP binding activity by approximately 50%, regardless of iron manipulation (*Online Supplementary Figure S5A*). Since low IRP activity predicts ferritin increase and TfR1 reduction, the results observed indicate that iron protein synthesis becomes IRP-independent in bortezomib-treated cells. At the transcriptional level, in *FTH* mRNA was increased approximately 3-fold upon bortezomib, irrespective of the iron status, while *TFR1* mRNA was reduced (*Online Supplementary Figure S5B* and *C*). Thus, *FTH* and *TFR1* mRNA were discordant with their corresponding protein levels in all the cell lines studied, with the exception of FtH in U266 cells.

We then evaluated protein synthesis and turnover. In MM.1S, KMS-18 and RPMI-8226, bortezomib blocked FtH increase in response to iron (Figure 2C). Only in U266 did bortezomib enhance *de novo* FtH synthesis, regardless of iron status (Figure 2C). Bortezomib supplementation did not increase TfR1 synthesis (*data not shown*), but delayed its turnover (Figure 2D).

Inadequate FtH levels mediate both the sensitivity to bortezomib and to iron toxicity

To confirm the role of FtH in bortezomib response, we silenced *FTH* gene expression in RPMI-8226 and U266 cells by shRNA. We generated RPMI-8226-29 and U266-29 cell lines, in which *FTH* mRNA was reduced by 50%-70% and FtH protein by 25/30% with respect to cells infected with scramble control shRNA (*Online Supplementary Figure S6A*). Cells with reduced FtH levels were more sensitive to bortezomib than control cells, as measured by MTT (Figure 3A) or by the increase in both AnV positive (early apoptotic) and AnV-PI double positive (late apoptotic) cells (Figure 3B). The strongest sensitization occurred for RPMI-8226-29, in which IC50 was reduced from 40 nM to 6 nM (Figure 3A).

As a further strategy to suppress FtH, we pre-incubated cells with DFO to induce iron depletion before adding bortezomib. Iron starvation strongly reduced ferritin levels and subsequent iron supplementation failed to increase FtH in all bortezomib-treated cells, including U266 (*Online Supplementary Figure S6B*). Pre-treatment with the iron chelator enhanced bortezomib sensitivity in all cell lines, as documented by increased early apoptotic cells (Figure 3C and D). Subsequent iron addition either as FeTf, FAC or FAC-NAC favored cell death, as shown by the increased percentage of AnV-PI double positive cells in MM.1S, KMS-18 and U266, being FAC-NAC the most effective combination (Figure 3C and D) (*Online Supplementary Figure S7*).

Iron sensitizes primary plasma cells to bortezomib

We investigated whether FtH reduction and iron supplementation enhanced the effect of bortezomib also in primary bone marrow-derived plasma cells of MM patients. Bone marrow CD138 positive (plasma cells) and CD138 negative fractions were treated with bortezomib with or without iron supplementation (*Online Supplementary Table S1*). As expected, the viability of plasma cells isolated from their microenvironment was highly compromised. Nevertheless, we could measure the increase of AnV-PI double positive cells after bortezomib plus FAC as compared with cells treated with bortezomib alone (Figure 4A and *Online Supplementary Figure S8*). In a further set of experiments, we analyzed cell viability by Trypan blue exclusion assay in cells pre-treated with the iron chelator DFO before adding bortezomib or bortezomib plus FAC.

DFO pre-treatment followed by FAC increased cell death in resistant (n=2 cases) CD138 positive cells (*Online Supplementary Tables S1 and S2*), while it was ineffective in CD138 negative fractions (Figure 4B).

To confirm the role of ferritin in primary plasma cells, we incubated cellular extracts *in vitro* with an excess of ^{55}FeAC in the presence of ascorbic acid. In this experimental condition, iron incorporation into ferritins measured by autoradiography is proportional to the ferritin protein content.[19] DFO pre-treatment reduced ferritin band intensity in all cell fractions. However, after bortezomib supplementation, ferritins were correctly up-regulated by iron only in the CD138 negative fraction (Figure 4C), while in the CD138 positive cells ferritin upregulation was abolished (Figure 4C). We concluded that the same mechanisms that explain sensitivity to iron toxicity upon bortezomib in cell lines are effective also in MM plasma cells *ex vivo*.

Discussion

Iron is essential for cell function and growth both in physiological and pathological conditions. Poor iron availability reduces the rate of cell replication,[20] and increased iron export from malignant cells correlates with better prognosis, as recently shown in breast cancer.[21] Iron excess is potentially toxic through its redox properties; however, normal cells limit these detrimental effects, reducing iron uptake and safely storing it into ferritin. The evidence that iron storage capacity directly correlates with resistance to the proteasome inhibitor bortezomib in MM cells suggests that manipulation of iron homeostasis might be exploited to increase the efficacy of the current therapies based on proteasome inhibition.

Ferritin and bortezomib sensitivity

The balance between proteasomal workload and capacity is critical to determine the sensitivity of MM cells to proteasomal inhibitors.[22] We found that also basal FtH levels contribute to bortezomib-sensitivity. FtH is the active catalytic subunit of cytosolic ferritin and the most abundant ferritin subunit in MM cell lines as FtH/FtL ratio measured in MM.1S, KMS-18, RPMI-8226 and U266 was approximately 20:1 (*data not shown*). As MM cells are particularly sensitive to redox imbalance,[23] high ferritin levels may protect MM cells from bortezomib-induced ROS generation by limiting free iron availability. Interestingly,

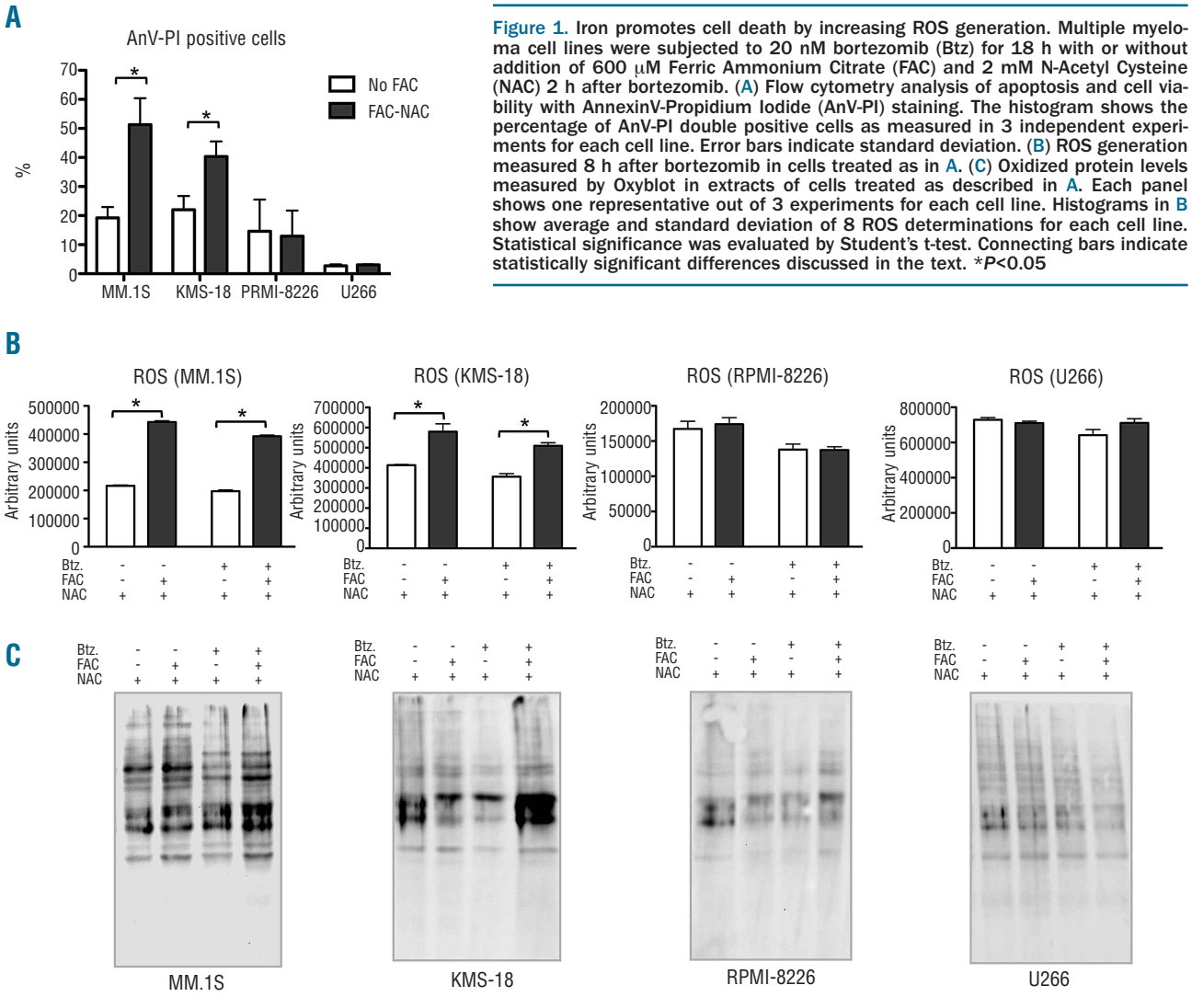

Figure 1. Iron promotes cell death by increasing ROS generation. Multiple myeloma cell lines were subjected to 20 nM bortezomib (Btz) for 18 h with or without addition of 600 μM Ferric Ammonium Citrate (FAC) and 2 mM N-Acetyl Cysteine (NAC) 2 h after bortezomib. (A) Flow cytometry analysis of apoptosis and cell viability with AnnexinV-Propidium Iodide (AnV-PI) staining. The histogram shows the percentage of AnV-PI double positive cells as measured in 3 independent experiments for each cell line. Error bars indicate standard deviation. (B) ROS generation measured 8 h after bortezomib in cells treated as in A. (C) Oxidized protein levels measured by Oxyblot in extracts of cells treated as described in A. Each panel shows one representative out of 3 experiments for each cell line. Histograms in B show average and standard deviation of 8 ROS determinations for each cell line. Statistical significance was evaluated by Student's t-test. Connecting bars indicate statistically significant differences discussed in the text. *P<0.05

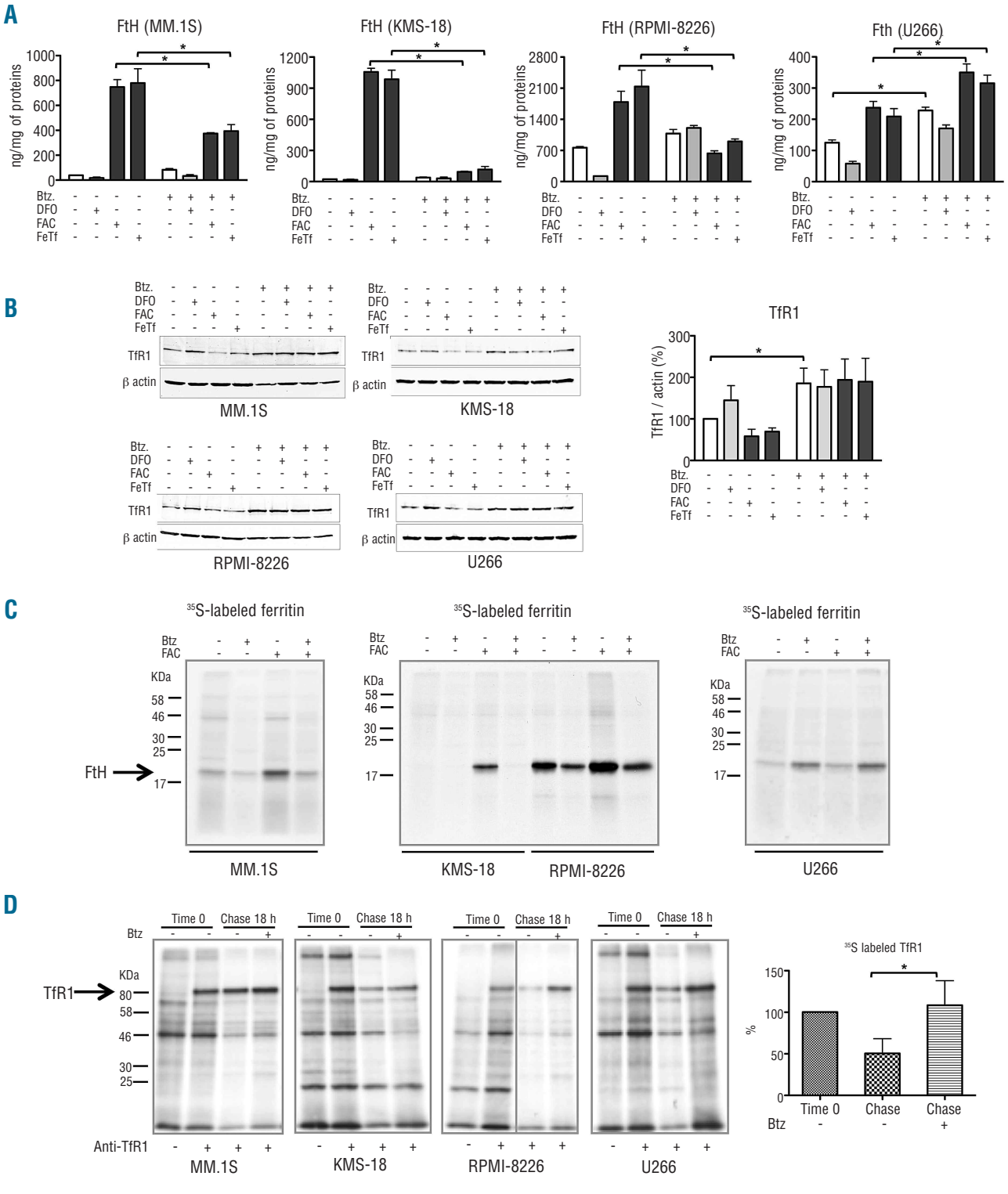

Figure 2. Bortezomib (Btz) deregulates the co-ordinated expression of iron proteins. Iron protein homeostasis in multiple myeloma cell lines subjected to Btz for 18 h. Iron concentration was modulated 2 h after bortezomib either by adding 300 μM Ferric Ammonium Citrate (FAC) or 40 μM transferrin bound iron (FeTf) or 100 μM of iron chelator deferoxamine (DFO). (A) Ferritin H (FtH) content assayed by ELISA. Panels show one representative out of 3 experiments for each cell line. (B) Transferrin Receptor 1 (TfR1) levels assayed by Western blotting (WB). Pictures show one representative WB for each cell line and histogram shows the TfR1 quantification as obtained by densitometry normalized on β-actin in 2 independent experiments for each cell line. (C) FtH protein synthesis. Cells were subjected to bortezomib and to 300 μM FAC in presence of radiolabeled 35S-Cys-Met amino acids mixture. Autoradiographies show representative results of immunoprecipitation with specific anti-FtH monoclonal antibody. The experiment was repeated three times for each cell line. (D) TfR1 protein turnover. Cells were loaded with radiolabeled 35S-Cys-Met aminoacids mixture and then subjected to bortezomib. Autoradiographies show representative results of immunoprecipitation with specific anti-TfR1 monoclonal antibody. The experiment was repeated twice in each cell line. The histogram shows TfR1 quantification as obtained by densitometry normalized on time point zero. Error bars indicate standard deviation. Statistical significance was evaluated by Student's t-test. Connecting bars indicate statistically significant differences discussed in the text. *$P<0.05$

in the most resistant U266 cell line, FtH increased in response to bortezomib. Consistent with a relevant role played by ferritin in bortezomib response, both the mild reduction in FtH expression obtained by shRNA, and the bigger reduction induced by DFO were able to sensitize cells to bortezomib. While DFO lowers both ferritin (FtH and FtL) subunits, the shRNA strategy confirmed the role of FtH in bortezomib resistance. Unfortunately, in this setting, such silencing has limited efficacy, since FtH regulation is mainly controlled post-trascriptionally by the IRE/IRP system. Thus, although FtH mRNA was silenced by 50%-70% upon shRNA infection, the corresponding protein was reduced by only 25%-30%, likely because the IRE/IRP system adjusted its translation according to cellu-

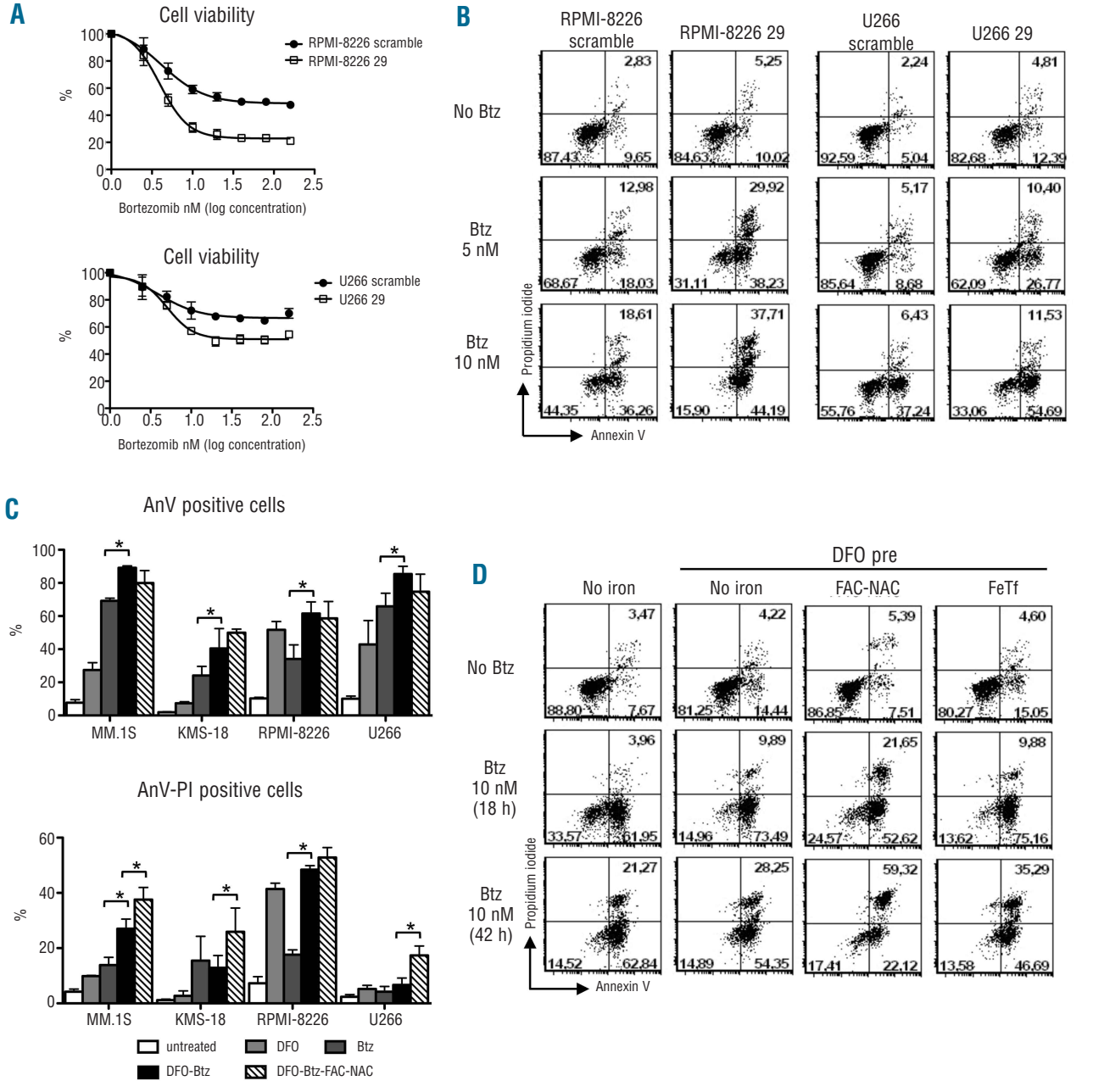

Figure 3. Cell viability of multiple myeloma cell lines treated with bortezomib (Btz) or bortezomib and iron after reduction of Ferritin H (FtH) protein levels. (A and B) FtH was reduced in RPMI-8226 and U266 cell lines by infection with specific shRNA against FtH (oligo-29) or with unspecific (scramble) shRNA. Cell viability was analyzed by (A) reduction of 3-(4,5-Dimethylthiazol-2-yl)-2,5-diphenyltetrazolium bromide (MTT) in cells subjected to bortezomib increasing concentration from 2.5 to 160 nM for 18 h, or by (B) flow cytometry analyses with AnnexinV-Propidium Iodide (AnV-PI) staining in cells subjected to 5 or 10 nM bortezomib for 18 h. Pictures show one representative out of 2 experiments for each cell line. (C and D) FtH was down-regulated by DFO pre-treatment (DFO pre). (C) Percentage of AnnexinV (AnV) positive and AnV-PI double positive cells after treatment with 10 nM bortezomib for 18 h with or without 600 μM Ferric Ammonium Citrate (FAC) and 2 mM N-Acetyl Cysteine (NAC). Histograms show average and standard deviation of 3 independent experiments for each cell line. (D) Representative flow cytometry analysis of U266 cell line. FeTf: transferrin bound iron (80 μM). Statistical significance was evaluated by Student's t-test. Connecting bars indicate statistically significant differences discussed in the text. *P<0.05.

lar needs. Actually, strong reduction in ferritin, as induced by DFO, was toxic by itself, particularly in RPMI-8226 cells characterized by high basal ferritin levels. This emphasizes the essential role of ROS buffering played by ferritin and reveals a crucial role of iron metabolism in MM cells.

Iron and bortezomib sensitivity

We proved that iron supplementation exaggerates toxicity in bortezomib-treated cells mainly by accelerating cell death of early apoptotic cells. Toxicity inversely correlated with basal ferritin level, a finding most evident in MM.1S and KMS-18, than in U266 and only slightly visible in RPMI-8226. Toxicity increases when ferritin was down-regulated by DFO. This occurred in all cells with the exception of the RPMI-8226, possibly because the high toxicity induced by the combination of DFO plus bortezomib covered any additional effect.

The MM cell lines studied have different basal levels of ferritin and TfR1. Still, they all correctly responded to iron supplementation with a concordant modulation of iron import and storage proteins. This regulation was lost after bortezomib treatment. As a consequence of the reduced iron storage capacity, ROS generation is not limited and

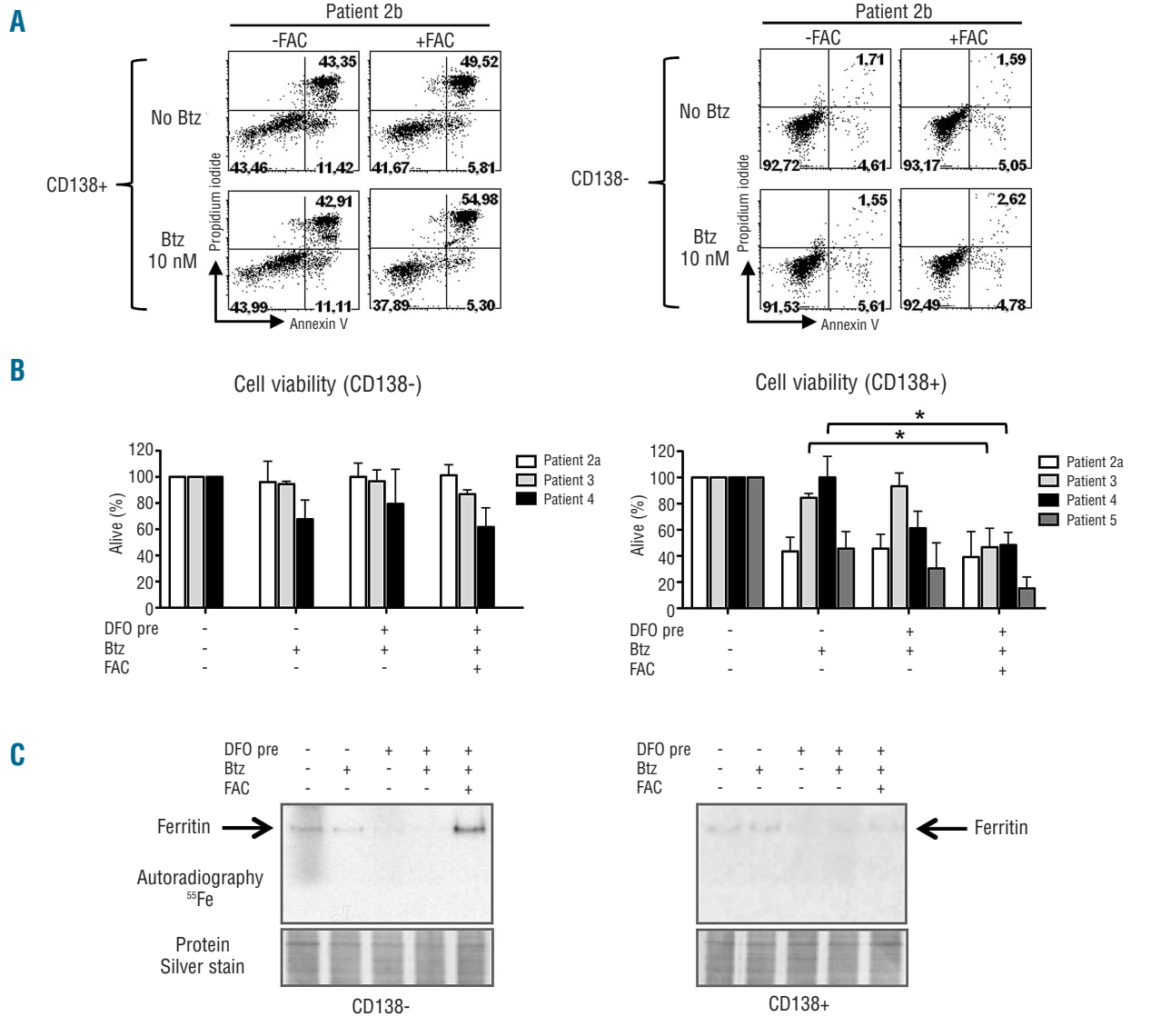

Figure 4. Iron sensitizes primary plasma cells to bortezomib. (A) Flow cytometry analysis of apoptosis and cell viability with AnnexinV-Propidium Iodide staining in CD138 positive and negative cells isolated from Patient 2 (sample b). Cells were subjected to 10 nM bortezomib (Btz) for 18 h and to 300 μM Ferric Ammonium Citrate (FAC) 2 h after bortezomib. (B) Cell viability was assayed by Trypan Blue exclusion assay in cells isolated from Patients 2 (sample a), 3, 4 and 5. Cells were treated with 100 μM of the iron chelator deferoxamine (DFO pre) to reduce ferritin levels and then subjected to 15 nM bortezomib and to 300 μM FAC for 18 h. Histograms display the percentage of viable cells corrected for basal cell viability to show the percentage of cell death induced by bortezomib alone or by the combined treatments (Detailed results are reported in *Online Supplementary Table S2*). Error bars indicate standard deviation. Statistical significance was evaluated by Student's t-test. Connecting bars indicate statistically significant differences discussed in the text. *$P<0.05$ (C) Ferritin content in primary cells treated as in B. Cellular extracts were incubated with ^{55}FeAC molar excess and then loaded into gel, without heating. Silver staining is shown to confirm equal protein loading. The experiment was performed on the cellular extracts from the bortezomib resistant cells of Patients 3 and 4. Pictures show representative autoradiographies. Arrows point to the band corresponding to ferritin.

iron toxicity synergizes with bortezomib to increase cell death. In all cells, we observed the strongest iron toxicity when we used FAC in combination with the antioxidant agent NAC. Actually, FAC is a good ferric iron source as it is stable at a neutral pH but it is slowly incorporated into cells. On the contrary, NAC is very efficiently taken up by cells. We speculate that, as a sulphhydryl compound, NAC might chelate metal ions, favoring iron incorporation. Alternatively, NAC could reduce ferric into ferrous iron, a more reactive iron source. In both cases, since we used high iron concentration, these events exceeded NAC antioxidant properties. The antioxidant properties were evident when iron was supplemented at a lower concentration and bound to its physiological carrier protein transferrin.

Our experimental conditions induced incorporation of great amounts of iron in all cells, even in bortezomib-untreated cells, as shown by the strong increase in ferritin. Thus, although stabilization of TfR1 by bortezomib might likely promote some additional iron up take, the inability to increase the iron storage capacity appears more crucial than iron import to explain iron toxicity upon bortezomib. Indeed, this toxicity was evident when iron was supplemented after bortezomib but was not observed when iron was supplemented before or concomitant with bortezomib (*data not shown*), since the intact homeostatic mechanism counteracted the detrimental effect of bortezomib and ROS by increasing ferritin. We concluded that, although bortezomib affects both iron import and storage proteins, the derangement of the latter mechanism caused most of the toxic effects.

Regulation of iron proteins

In the absence of bortezomib, iron supplementation did not affect cell viability, as expected from the ability of cells to tightly regulate iron homeostasis and buffer ROS formation. This response requires the co-ordinated reduction in TfR1 together with the increase in ferritin and, in some cases, in ferroportin, to decrease iron uptake and favor iron storage and export, respectively. Since protein expression in response to iron is controlled by IRP, we asked whether IRP were responsible for TfR1 and ferritin deregulation. Our findings revealed that bortezomib strongly impaired the IRP binding activity, which remained lower than baseline also after DFO-induced iron depletion. This impairment could be determined by the oxidative stress generated by bortezomib, since low IRP binding occurs after long exposure to oxidative stimuli.[24]

The abundance of TfR1 in bortezomib-treated cells, despite low levels of cognate mRNA, could be ascribed to reduced protein degradation, possibly as a direct consequence of proteasome inhibition.[25] Low ferritin, however, despite high levels of cognate mRNA, could be the result of the overall reduction of protein translation that occurs after bortezomib (*data not shown*), likely as a consequence of UPR or other stresses entailing eIF2α phosphorylation.[26] Within this general event, the inability to translate ferritin becomes specifically dangerous after iron supplementation, rendering the cells vulnerable to ROS damage. Impaired FtH translation did not occur in the resistant U266 cells. We speculate that bortezomib was unable to promote a stress response sufficient to affect FtH synthesis in these cells. Their ability to increase *FtH* protein further contributed to the resistant phenotype. Accordingly, bortezomib was able to prevent ferritin accumulation only in U266 cells when their basal ferritin levels were reduced by DFO pre-treatment.

Iron toxicity in primary MM cells

Our data disclose a potential Achille's heel (iron susceptibility during proteasomal inhibition) in MM cell lines. The same phenomenon occurs also in primary cells. Although isolation from the microenvironment affected the viability of CD138 positive cells in our experimental model *in vitro* we were able to determine a range of sensitivity to bortezomib similar to that observed in patient follow up (*Online Supplementary Table S1*). Interestingly, neither the bortezomib concentrations used nor the DFO-bortezomib-iron protocol affected the CD138 negative cells that maintained ferritin homeostasis, preventing iron toxicity.

From a general therapeutic perspective, interfering with iron homeostasis emerges as a potential strategy to enhance proteasomal inhibitory effects in MM. To overcome resistance, the challenge remains as to how to selectively reduce ferritin levels of malignant plasma cells, to induce apoptosis upon bortezomib, and how to further supplement iron to accelerate the death of early apoptotic cells. We speculate that the high IL-6 levels in the MM microenvironment[27] sequesters iron in macrophages through an autocrine mechanism induced by local hepcidin overproduction.[28] In the bone marrow this would amplify the hepcidin systemic effect that leads to iron sequestration, iron restricted erythropoiesis, and anemia of chronic diseases in patients.[29] Hepcidin antagonists and novel inflammatory modulators are promising players in the future design of new treatment strategies.[30] Removing iron has been proposed as a mechanism to induce cancer cell death. Our data indicate that, according to the biology of the tumor cells, increasing iron concentration could be of potential benefit as well.

Acknowledgments

The authors would like to thank Fabio Ciceri, Cristina Tresoldi, Roberta Orlandi and Elena Antonini for providing plasma cells of MM patients. We thank Sonia Levi for helpful discussion.

Funding

This work was supported by the Program Grant in Molecular Oncology n. 9965 Associazione Italiana Ricerca sul Cancro 5 per 1000, Milano, Italy.

Authorship and Disclosures

Information on authorship, contributions, and financial & other disclosures was provided by the authors and is available with the online version of this article at www.haematologica.org.

References

1. Maes K, Nemeth E, Roodman GD, Huston A, Esteve F, Freytes C, et al. In anemia of multiple myeloma, hepcidin is induced by increased bone morphogenetic protein 2. Blood. 2010;116(18):3635-44.
2. Katodritou E, Ganz T, Terpos E, Verrou E, Olbina G, Gastari V, et al. Sequential evaluation of serum hepcidin in anemic myeloma patients: study of correlations with myeloma treatment, disease variables, and anemia response. Am J Hematol. 2009; 84(8):524-6.
3. Hentze MW, Muckenthaler MU, Galy B, Camaschella C. Two to tango: regulation of Mammalian iron metabolism. Cell.

2010;142(1):24-38.
4. Wang J, Pantopoulos K. Regulation of cellular iron metabolism. Biochem J. 2011;434 (3):365-81.
5. Garrick MD. Human iron transporters. Genes and nutrition. 2011;6(1):45-54.
6. Arosio P, Levi S. Cytosolic and mitochondrial ferritins in the regulation of cellular iron homeostasis and oxidative damage. Biochim Biophys Acta. 2010;1800(8):783-92.
7. Recalcati S, Minotti G, Cairo G. Iron regulatory proteins: from molecular mechanisms to drug development. Antioxid Redox Sign. 2010;13(10):1593-616.
8. Chauhan D, Hideshima T, Anderson KC. Proteasome inhibition in multiple myeloma: therapeutic implication. Annu Rev Pharmacol. 2005;45:465-76.
9. Richardson PG, Barlogie B, Berenson J, Singhal S, Jagannath S, Irwin D, et al. A phase 2 study of bortezomib in relapsed, refractory myeloma. New Engl J Med. 2003;348(26):2609-17.
10. Richardson PG, Mitsiades C, Hideshima T, Anderson KC. Bortezomib: proteasome inhibition as an effective anticancer therapy. Annu Rev Med. 2006;57:33-47.
11. Rouault TA. The role of iron regulatory proteins in mammalian iron homeostasis and disease. Nat Chem Biol. 2006;2(8):406-14.
12. Wang J, Fillebeen C, Chen G, Biederbick A, Lill R, Pantopoulos K. Iron-dependent degradation of apo-IRP1 by the ubiquitin-proteasome pathway. Mol Cell Biol. 2007; 27(7):2423-30.
13. Matsunaga T, Kotamraju S, Kalivendi SV, Dhanasekaran A, Joseph J, Kalyanaraman B. Ceramide-induced intracellular oxidant formation, iron signaling, and apoptosis in endothelial cells: protective role of endogenous nitric oxide. J Biol Chem. 2004;279 (27):28614-24.
14. Kotamraju S, Kalivendi S, Shang T, Kalyanaraman B. Nitric oxide, proteasomal function, and iron homeostasis--implications in aging and neurodegenerative diseases. Methods Enzymol. 2005;396:526-34.
15. Zhang Y, Mikhael M, Xu D, Li Y, Soe-Lin S, Ning B, et al. Lysosomal proteolysis is the primary degradation pathway for cytosolic ferritin and cytosolic ferritin degradation is necessary for iron exit. Antioxid Redox Sign. 2010;13(7):999-1009.
16. De Domenico I, Vaughn MB, Li L, Bagley D, Musci G, Ward DM, et al. Ferroportin-mediated mobilization of ferritin iron precedes ferritin degradation by the proteasome. Embo J. 2006;25(22):5396-404.
17. De Domenico I, Ward DM, Kaplan J. Specific iron chelators determine the route of ferritin degradation. Blood. 2009;114 (20):4546-51.
18. Cozzi A, Rovelli E, Frizzale G, Campanella A, Amendola M, Arosio P, et al. Oxidative stress and cell death in cells expressing L-ferritin variants causing neuroferritinopathy. Neurobiol Dis. 2010;37(1):77-85.
19. Cozzi A, Corsi B, Levi S, Santambrogio P, Albertini A, Arosio P. Overexpression of wild type and mutated human ferritin H-chain in HeLa cells: in vivo role of ferritin ferroxidase activity. J Biol Chem. 2000;275 (33):25122-9.
20. Yu Y, Richardson DR. Cellular iron depletion stimulates the JNK and p38 MAPK signaling transduction pathways, dissociation of ASK1-thioredoxin, and activation of ASK1. J Biol Chem. 2011;286(17):15413-27.
21. Pinnix ZK, Miller LD, Wang W, D'Agostino R Jr, Kute T, Willingham MC, et al. Ferroportin and iron regulation in breast cancer progression and prognosis. Sci Transl Med. 2010;2(43):43ra56.
22. Bianchi G, Oliva L, Cascio P, Pengo N, Fontana F, Cerruti F, et al. The proteasome load versus capacity balance determines apoptotic sensitivity of multiple myeloma cells to proteasome inhibition. Blood. 2009;113(13):3040-9.
23. Nerini-Molteni S, Ferrarini M, Cozza S, Caligaris-Cappio F, Sitia R. Redox homeostasis modulates the sensitivity of myeloma cells to bortezomib. Br J Haematol. 2008;141(4):494-503.
24. Tsuji Y, Ayaki H, Whitman SP, Morrow CS, Torti SV, Torti FM. Coordinate transcriptional and translational regulation of ferritin in response to oxidative stress. Mol Cell Biol. 2000;20(16):5818-27.
25. Kotamraju S, Tampo Y, Keszler A, Chitambar CR, Joseph J, Haas AL, et al. Nitric oxide inhibits H2O2-induced transferrin receptor-dependent apoptosis in endothelial cells: Role of ubiquitin-proteasome pathway. Proc Natl Acad Sci USA. 2003;100(19):10653-8.
26. Obeng EA, Carlson LM, Gutman DM, Harrington WJ Jr, Lee KP, Boise LH. Proteasome inhibitors induce a terminal unfolded protein response in multiple myeloma cells. Blood. 2006;107(12):4907-16.
27. van Zaanen HC, Koopmans RP, Aarden LA, Rensink HJ, Stouthard JM, Warnaar SO, et al. Endogenous interleukin 6 production in multiple myeloma patients treated with chimeric monoclonal anti-IL6 antibodies indicates the existence of a positive feedback loop. J Clin Invest. 1996;98(6):1441-8.
28. Theurl I, Theurl M, Seifert M, Mair S, Nairz M, Rumpold H, et al. Autocrine formation of hepcidin induces iron retention in human monocytes. Blood. 2008;111(4): 2392-9.
29. Weiss G, Goodnough LT. Anemia of chronic disease. New Engl J Med. 2005;352(10): 1011-23.
30. Cullis JO. Diagnosis and management of anaemia of chronic disease: current status. Br J Haematol. 2011;154(3):289-300.